Quaternary Lidocaine Derivative QX-314 Activates and Permeates Human TRPV1 and TRPA1 to Produce Inhibition of Sodium Channels and Cytotoxicity

Thomas Stueber, M.D., Mirjam J. Eberhardt, M.D., Christoph Hadamitzky, M.D., Annette Jangra, Cand.Med., Stefan Schenk, Cand.Med., Felicia Dick, Cand.Med., Carsten Stoetzer, M.D., Katrin Kistner, Ph.D., Peter W. Reeh, M.D., Ph.D., Alexander M. Binshtok, Ph.D., Andreas Leffler, M.D.

ABSTRACT

Background: The relatively membrane-impermeable lidocaine derivative QX-314 has been reported to permeate the ion channels transient receptor potential vanilloid 1 (TRPV1) and transient receptor potential cation channel, subfamily A, member 1 (TRPA1) to induce a selective inhibition of sensory neurons. This approach is effective in rodents, but it also seems to be associated with neurotoxicity. The authors examined whether the human isoforms of TRPV1 and TRPA1 allow intracellular entry of QX-314 to mediate sodium channel inhibition and cytotoxicity.

Methods: Human embryonic kidney 293 (HEK-293) cells expressing wild-type or mutant human (h) TRPV1 or TRPA1 constructs as well as the sodium channel Nav1.7 were investigated by means of patch clamp and ratiometric calcium imaging. Cytotoxicity was examined by flow cytometry.

Results: Activation of hTRPA1 by carvacrol and hTRPV1 by capsaicin produced a QX-314–independent reduction of sodium current amplitudes. However, permeation of QX-314 through hTRPV1 or hTRPA1 was evident by a concentration-dependent, use-dependent inhibition of Nav1.7 activated at 10 Hz. Five and 30 mM QX-314 activated hTRPV1 *via* mechanisms involving the intracellular vanilloid-binding domain and hTRPA1 *via* unknown mechanisms independent of intracellular cysteins. Expression of hTRPV1, but not hTRPA1, was associated with a QX-314–induced cytotoxicity (viable cells 48 ± 5% after 30 mM QX-314) that was ameliorated by the TRPV1 antagonist 4-(3-chloro-2-pyridinyl)-*N*-[4-(1,1-dimethylethyl)phenyl]-1-piperazinecarboxamide (viable cells 81 ± 5%).

Conclusions: The study data demonstrate that QX-314 directly activates and permeates the human isoforms of TRPV1 and TRPA1 to induce inhibition of sodium channels, but also a TRPV1-dependent cytotoxicity. These results warrant further validation of this approach in more intact preparations and may be valuable for the development of this concept into clinical practice. **(Anesthesiology 2016; 124:1153-65)**

LOCAL anesthetics are unselective inhibitors of voltage-gated sodium channels and accordingly they induce an unselective block of sensory and motor neurons.[1] Binshtok *et al.*[2] demonstrated that the quaternary lidocaine derivative QX-314 induces a preferential nociceptive block, presumably by permeating through the channel pore of the capsaicin receptor transient receptor potential vanilloid 1 (TRPV1). This effect of QX-314 was reproduced in preclinical studies in rodents,[3–8] and more recent studies indicate that QX-314 can also permeate the pore of transient receptor potential cation channel, subfamily A, member 1 (TRPA1).[3,9,10] Other reports document that QX-314 also induces a strong and long-lasting motor block,[11] that is, an inhibition of nerve fibers lacking TRPV1 and TRPA1. Intriguingly, it was recently demonstrated that QX-314 can also block myelinated A-fibers by permeating through the Toll-like receptor 5.[12] Nevertheless, a possible approach to establish a preferential and long-lasting sensory nerve block is to guide poorly membrane-permeable sodium

What We Already Know about This Topic

- The poorly cell-penetrating lidocaine analog QX-314 can gain access to nociceptor sensory nerves by entry through pain-related ion channels (TRPV1 and TRPA1) to produce selective inhibition of just pain fibers but can also cause toxicity

What This Article Tells Us That Is New

- In cells expressing human TRPV1 and TRPA1 channels, QX-314 activates both channels and enters the cell to inhibit sodium currents
- In these cells QX-314 produces cytotoxicity by a mechanism dependent on TRPV1 channels

Parts of this study have been presented as a short presentation at the "Wissenschaftliche Arbeitstage der DGAI" on February 28, 2015, in Wuerzburg, Germany, and as a poster at the "Deutsche Anästhesiecongress" on May 9, 2015, in Duesseldorf, Germany.

Submitted for publication May 7, 2015. Accepted for publication January 12, 2016. From the Department of Anaesthesiology and Intensive Care Medicine, Hannover Medical School, Hannover, Germany (T.S., M.J.E., C.H., A.J., S.S., F.D., C.S., A.L.); Department of Physiology and Pathophysiology, Friedrich-Alexander-Universität Erlangen-Nürnberg, Erlangen, Germany (K.K., P.W.R.); and Department of Medical Neurobiology, Institute for Medical Research Israel-Canada, The Hebrew University Faculty of Medicine, and The Edmond and Lily Safra Center for Brain Sciences, The Hebrew University, Jerusalem, Israel (A.M.B.).

 Anesthesiology 2016; 124:1153-65

<zdoi;10.1097/ALN.0000000000001050>

channel blockers through the pore of TRPV1 and TRPA1 mainly expressed in nociceptive sensory neurons. To our knowledge, permeation of QX-314 has not yet been demonstrated for human (h) TRPV1 or TRPA1. Several studies have demonstrated that the human isoforms of both TRPV1 and TRPA1 display pronounced differences in terms of function and pharmacology compared with the rodent isoforms.[13–19] If the concept of the permeation of QX-314 through TRP channels is to be translated into clinical practice, it seems mandatory to define the effects of QX-314 on hTRPV1 and hTRPA1.

Perisciatic injection of QX-314 in combination with capsaicin resulted in profound neurotoxicity associated with nerve loss.[5] Moreover, intrathecal injection of QX-314 in mice results in severe irritation or even death.[20] Considering that a severe neurotoxic potential of QX-314 would prevent an introduction of this approach into clinical practice, defining the mechanisms mediating a QX-314–induced neurotoxicity seems indispensable. One possibility is that activation of TRPV1 and TRPA1 might trigger a calcium-dependent apoptosis or necrosis leading to cell death.[21,22] Recent studies demonstrated that local anesthetics induce calcium influx in sensory neurons by activating TRPV1 and TRPA1.[19,23–25] However, the jury is still out on whether QX-314 activates TRPV1. Although some reports find that QX-314 fails to activate rodent isoforms of both TRPV1 and TRPA1 due to its poor membrane permeability, a more recent study demonstrated that rat TRPV1 (rTRPV1) can generate membrane currents when challenged by QX-314 at millimolar concentrations.[7,19,25] It is therefore possible that human TRPV1 and TRPA1 are involved in QX-314–induced neurotoxicity either by channel activation or by entry of QX-314 through the channel pore.

In the current study, we aimed to investigate the interaction of QX-314 with hTRPV1 and hTRPA1 with regard to permeation with subsequent inhibition of sodium channels as well as a possible direct channel activation mediating calcium influx and possibly cytotoxicity. We used human embryonic kidney 293 (HEK-293) cells with stable or transient expression of either hTRPV1 or hTRPA1 together with the sodium channel α-subunit Nav1.7. The effects of QX-314 on these ion channels were examined with whole cell patch clamp as well as ratiometric calcium imaging recordings. Cell viability was examined by flow cytometry after double staining with propidium iodide (PI) and annexin V.

Materials and Methods

Chemicals

QX-314 (lidocaine-*N*-ethyl chloride) and lidocaine (both from Sigma-Aldrich, Germany) were directly dissolved in water or cell culture medium depending on experiments. 4-(3-Chloro-2-pyridinyl)-*N*-[4-(1,1-dimethylethyl)phenyl]-1-piperazinecarboxamide (BCTC), a TRPV1 antagonist, HC-030031, a TRPA1 antagonist (both from Tocris, United Kingdom), and the TRPA1 agonists carvacrol and acrolein (both from Sigma-Aldrich) were dissolved in dimethylsulfoxide (DMSO). The TRPV1 agonist capsaicin (Biotrend, Germany) was dissolved in ethanol. All stock solutions were stored at −20°C and diluted into appropriate test concentrations in extracellular buffer solution or cell culture medium before the experiments.

Cell Culture

Stable hTRPV1-HEK-293 cells (a kind gift from Dr. Peter Zygmunt, Lund, Sweden), hTRPA1-HEK-293 cells, and HEK-293t cells were cultured in standard Dulbecco's modified Eagle medium (D-MEM, Gibco, BRL Life Technologies, Germany) with 10% fetal bovine serum (Biochrom, Germany), 100 U/ml penicillin, 100 μg/ml streptomycin (Gibco), and 2 mM Glutamax (Gibco). Five micrograms per milliliter of blasticidin (PAA, Austria) and 0.35% Zeocin (Invitrogen, France) were added for stable expression of hTRPV1, and for induction, tetracycline (Sigma-Aldrich) 0.1 μg/ml was added to the medium 16 to 24 h before the experiments. A stable hTRPA1-HEK-293 cell line was established by using G418 800 μg/ml (both from Sigma-Aldrich) as described previously.[18] Cells were cultivated at 37°C and 5% CO_2 in Petri dishes (Greiner Bio-One, Germany) or 12-well plates (Thermo Fisher Scientific, Germany) 12 to 24 h before the experiments. For transient transfection of HEK-293t cells or the stable cell lines, complementary DNA of rTRPV1 (a kind gift from Dr. David Julius, San Francisco, California), mouse TRPA1 (a kind gift from Dr. Ardem Patapoutian, San Diego, California), rabbit TRPV1 (oTRPV1) and the o/rTRPV1-chimera (kind gifts from Dr. Narender Gavva, Amgen Inc., Thousand Oaks, California), hTRPA1-C621S/C641S/C665S (hTRPA1–3C, kindly provided by Dr. Sven-Eric Jordt, New Haven, Connecticut), or human Nav1.7 (hNav1.7, kindly provided by Dr. Angelika Lampert, Aachen, Germany) was cotransfected with 0.5 μg plasma for enhanced green fluorescent protein (Clontech, USA) by using a nanofectin transfection kit according to the instructions of the manufacturer (PAA). All experiments were performed in accordance with the requirements of the local authorities (Gewerbeaufsicht, Niedersachsen, Germany).

Electrophysiology

Whole cell patch clamp experiments were carried out with a HEKA Electronics USB 10 amplifier and the Patchmaster software (HEKA Electronics, Germany). Borosilicate pipettes with a resistance of 1 to 2 MΩ were filled with a pipette solution containing 140 mM KCl, 2 mM $MgCl_2$, 5 mM EGTA, and 10 mM HEPES with pH adjusted to 7.4 by KOH. Standard extracellular solution contained 140 mM NaCl, 5 mM KCl, 2 mM $MgCl_2$, 1.2 mM $CaCl_2$, 10 mM HEPES, and 10 mM glucose with pH 7.4 adjusted by tetramethylammonium hydroxide (TMA-OH). Calcium-free extracellular solution contained 140 mM NaCl, 5 mM KCl, 2 mM $MgCl_2$, 5 mM EGTA, 10 mM HEPES, and 10 mM glucose with pH adjusted to 7.4 by TMA-OH. Transfected cells were visualized

by enhanced green fluorescent protein fluorescence before the recording. Only one cell per dish was used for experiments. For sodium currents, data were sampled at 25 kHz and filtered at 5 kHz. The series resistance was compensated by 60 to 80%, and the capacitance artifacts were cancelled using the Patchmaster software. For experiments on tonic block of sodium currents, linear leak subtraction based on resistance estimates from four hyperpolarizing pulses applied after depolarizing test potential was used. For TRPV1- and TRPA1-mediated membrane currents, data were sampled at 10 kHz and filtered at 2 kHz. All substances were applied by a gravity-driven perfusion system allowing a focal application of test solution within a distance of less than 100 µm from the cell. The Fitmaster software (HEKA Electronics) and Origin 8.5.1 software (Origin Lab, USA) were used for data analysis. The availability curves were generated from a double-pulse protocol described in detail in figure 1. Data were fitted by the Boltzmann equation ($y = 1/\{1 + \exp(EPP - 0.5)/k_h\}$), where EPP is a conditioning pulse potential, 0.5 is the voltage at which $y = 0.5$, and k_h is the slope factor. To obtain the IC_{50} value for tonic block by lidocaine, peak current amplitudes at different drug concentrations were normalized to the value obtained in control solution. Data were fitted with the Hill equation $y = y_{max} \times \{(IV_{50}n / IC_{50}n \times Cn)\}$, where y_{max} is the maximal amplitude, IC_{50} is the concentration at which $y/y_{max} = 0.5$, and n is the Hill coefficient.

Ratiometric $[Ca^{2+}]_i$ Measurements

Cells were filled by 4 µM fura-2-acetoxylmethyl ester (fura-2-AM) and 0.02% pluronic for approximately 45 min. After washout to allow fura-2-AM deesterification, coverslips were mounted on an inverse microscope with a 20X objective (Axio Observer D1; Zeiss, Germany). Cells were constantly superfused with extracellular solution containing 145 mM NaCl, 5 mM KCl, 1.25 mM $CaCl_2$, 1 mM $MgCl_2$, 10 mM glucose, and 10 mM HEPES by using a software-controlled, seven-channel, gravity-driven, common-outlet superfusion system. Fura-2 was excited using a microscope light source and an LEP filter wheel (Ludl Electronic Products Ltd., USA) to switch between 340- and 380-nm wavelength. Images were exposed for 20 and 40 ms, respectively, and acquired at a rate of 1 Hz with a CCD camera (Cool SNAP EZ; Photometrics, USA). Data were recorded using VisiView 2.1.1 software (Visitron Systems GmbH, Germany). Background fluorescence was subtracted before calculation of ratios. QX-314 was applied in concentrations of 5 and 30 mM for 40 s. To identify TRPV1- or TRPA1-expressing cells on a functional level, 0.3 µM capsaicin (10 s) and 100 µM acrolein (20 s) stimuli were used as positive control, and 5 µM ionomycin was applied as a control at the end of each experiment. Means (± SEM) of area under the curve (AUC) (delta ratio F340/380 nm) for regions of interest are presented.

Flow Cytometry

Cell viability was assessed by double staining with PI and fluorescein isothiocyanate (FITC) annexin V according to the protocol of the manufacturer (FITC Annexin V Apoptosis Detection Kit 1; BD Pharmingen, Germany) and as described before.[26] Cells were cultured in 12-well plates (Thermo Fisher Scientific) and exposed to tested substances for 15 min when reaching 80% confluency. Twenty-four hours after incubation, cells were detached using phosphate-buffered saline (PBS) and washed together with the corresponding supernatant with PBS. Cell pellets were resuspended in annexin V binding buffer (1X), and cell count was adjusted to 1×10^6/ml. One hundred microliters of the cell suspension was transferred into 5-ml polystyrene tubes (BD Pharmingen). Staining was performed by adding 5 µl PI and 5 µl annexin V. After incubation for 15 min at room temperature in the dark, 400 µl binding buffer (BD Pharmingen) was added. Specimens were analyzed within 1 h after staining by using a Cytomics FC500 flow cytometer (Beckmann Coulter, Germany). A total of 10,000 cells per sample were measured. Based on previous investigations, experiments were repeated three times. Data were analyzed with FlowJo version 10 (FlowJo LLC, USA).

Statistical Analysis

All data are presented as mean ± SD. Statistical analysis was performed by using GraphPad Prism 5 (GraphPad Software Inc., USA). Comparisons between two groups with different sample sizes were performed by nonparametric, two-tailed testing with the Mann–Whitney U test and between more than two groups with the Kruskal–Wallis test with Dunn *post hoc* correction. Multiple comparisons for groups with equal, balanced sample sizes were performed by ANOVA with a Tukey *post hoc* test. Significance was assumed for P value of 0.05 or less. Previous studies were used for estimation of sample sizes, that is, no formal *a priori* power analysis and sample size projection were performed.

Results

QX-314 Permeates hTRPV1 and hTRPA1 to Block Sodium Currents

To examine the effect of externally applied QX-314 on sodium current, we used HEK-293t cells expressing hNav1.7 and hTRPV1 channels. In order to examine tonic block, we evoked sodium currents by 40 depolarizing pulses from the holding potential of −70 mV to −10 mV at 0.1 Hz (fig. 1A). At this holding potential, however, we detected a strong rundown of the peak current amplitudes even in control solution (45 ± 28%, n = 23; fig. 1B). When the same protocol was used in cells held at −120 mV, the current amplitude even slightly increased over time (6 ± 10%; n = 25; fig. 1B). In order to find the optimal holding potential for the experiment, we further examined the voltage-dependent fast inactivation. Fast inactivation was induced by 100-ms-long prepulses ranging from −150 to −10 mV applied in

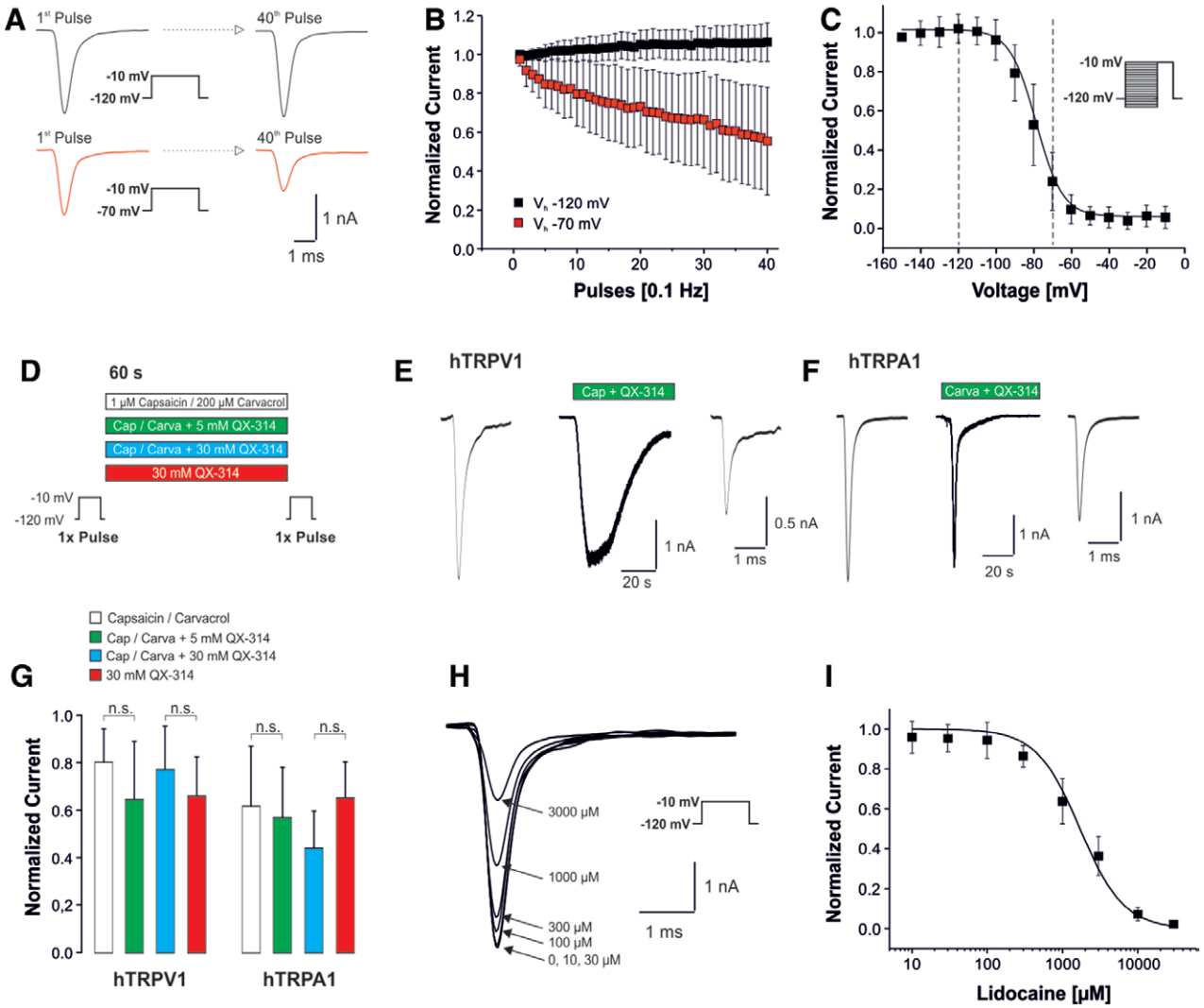

Fig. 1. Activation of human (h) transient receptor potential vanilloid 1 (TRPV1) and human transient receptor potential cation channel, subfamily A, member 1 (TRPA1) results in a QX-314–independent reduction of sodium current peak amplitudes. (*A*) Typical traces of sodium currents of Nav1.7 expressed in human embryonic kidney 293t (HEK-293t) cells. Currents were activated at 0.1 Hz by 40 test pulses from the holding potentials of −120 (*upper traces*) or 70 mV (*lower traces*) to −10 mV. (*B*) The averaged normalized peak current amplitudes of current activated from traces 1 to 40. Note that holding at −120 mV generated currents with stable peak amplitudes throughout the protocol, whereas currents generated in cells held at −70 mV underwent a strong rundown. (*C*) Voltage dependency of fast inactivation of Nav1.7 expressed in HEK-293t cells. *Inset*: the recording protocol; cells were held at −120 mV and fast inactivation was induced by 100-ms-long depolarizing test pulses applied in steps on 10 mV between −150 and −10 mV followed by a test pulse to −10 mV. Current amplitudes were normalized to the value obtained at −150 mV and plotted against the membrane potential. The *solid line* represents the Boltzmann fit and the *dotted lines* are drawn to guide eye for estimation of the fraction of inactivated channels at −120 and −70 mV. (*D*) Scheme of the protocol applied to determine inhibition of sodium currents after activation of hTRPV1 or hTRPA1 ± QX-314. Sodium currents were activated by test pulses from −120 to −10 mV before and after a 60-s-long application of 1 μM capsaicin, 1 μM capsaicin + 5 mM QX-314, 1 μM capsaicin + 30 mM QX-314, 200 μM carvacrol, 200 μM carvacrol + 5 mM QX-314, 200 μM carvacrol + 30 mM QX-314, or 30 mM QX-314 alone. (*E* and *F*) Representative current traces obtained using the protocol described in *D* from cells expressing hTRPV1 (5 mM QX-314 together with 1 μM capsaicin, *E*) and hTRPA1 (5 mM QX-314 together with 200 μM carvacrol, *F*). (*G*) Bar diagrams displaying the inhibition of sodium currents following protocols described in *D*. The peak amplitude of sodium currents activated after application of agonist ± QX-314 were normalized to the peak amplitudes of sodium currents determined before the protocol. Note that 5 mM QX-314 did not induce a significant reduction of sodium currents compared with the application of the classical agonists alone. (*H*) Representative traces of lidocaine-induced tonic block of resting Nav1.7 channels. Cells were held at −120 mV and currents were activated by test pulses to −10 mV at 0.1 Hz, and increasing concentrations of lidocaine were applied to induce tonic block. (*I*) The dose–response curve of lidocaine-induced tonic block of Nav1.7-mediated sodium currents. Current amplitudes determined at each concentration were normalized to the current activated in control solution and then plotted against the lidocaine concentration. The *solid line* represents the Hill fit (see Materials and Methods). Data are mean ± SD. n.s. = not significant.

steps of 10 mV (fig. 1C). The available current amplitude was then determined by a test pulse to −10 mV, normalized to the amplitude determined at −150 mV, and plotted against the corresponding voltage. Although a considerable fraction of channels are already inactivated at −70 mV, 100% are available at −120 mV (fig. 1C; see dotted lines, midpoint of steady-state inactivation: −79 ± 6 mV, n = 8). We therefore proceeded with protocols by which the sodium currents were monitored in cells held at −120 mV. Previous reports showed a prominent reduction of total sodium currents in rodent dorsal root ganglion cells after application of 5 mM QX-314 or higher.[2,8] As is demonstrated by the cartoon in figure 1D, cells expressing either hTRPV1 or hTRPA1 were treated with the following test solutions for 60 s: (1) 1 μM capsaicin or 200 μM carvacrol alone, (2) capsaicin (fig. 1E) or carvacrol (fig. 1F) in combination with 5 mM QX-314, (3) capsaicin or carvacrol in combination with 30 mM QX-314, or (4) 30 mM QX-314 alone. After application of any combination of substances, peak current amplitudes were reduced in both hTRPV1- and hTRPA1-expressing cells (fig. 1G). When compared with the reduction of the current amplitude by 1 μM capsaicin alone (20 ± 14%, n = 10), the coapplication of neither 5 mM QX-314 (35 ± 24%, n = 16) nor 30 mM QX-314 (23 ± 18%, n = 26, both $P > 0.05$, Kruskal–Wallis with *post hoc* Dunn test) resulted in a stronger inhibition in cells expressing hTRPV1. Furthermore, the effect of 30 mM QX-314 alone (34 ± 16%, n = 6) did not significantly differ from the effect induced by 30 mM QX-314 in combination with capsaicin ($P > 0.05$, Kruskal–Wallis with *post hoc* Dunn test). In hTRPA1-expressing cells, 200 μM carvacrol (38 ± 25%, n = 10) alone induced a similar reduction of sodium currents compared with the coapplication of carvacrol with QX-314 at both 5 mM (43 ± 21%, n = 20) and 30 mM QX-314 (56 ± 16%, n = 10) (both $P > 0.05$, Kruskal–Wallis with *post hoc* Dunn test). Again, the effect of 30 mM QX-314 alone (35 ± 15%, n = 8) did not significantly differ from the effect induced by 30 mM QX-314 in combination with carvacrol ($P > 0.05$, Kruskal–Wallis with *post hoc* Dunn test). These data suggest that application of QX-314 does not produce a robust additional blockade of sodium currents compared with application of capsaicin respectively carvacrol alone. It is possible that the amount of cytosolic QX-314 accumulation during 60 s was not enough to induce a robust tonic inhibition. To examine this notion, we determined tonic block of resting Nav1.7 channels (*i.e.*, holding potential of −120 mV) by lidocaine at concentrations from 10 to 30,000 μM (fig. 1, H and I). The calculated (see Hill equation in Materials and Methods) IC_{50} value for this tonic block was 1,710 ± 242 μM (n = 6 to 11 for each concentration). Assuming that cytosolic QX-314 and lidocaine should be more or less equipotent, this result indeed suggests that very high concentrations of QX-314 need to accumulate in the cytosol in order to induce a substantial inhibition of resting sodium channels. It was previously demonstrated that longer application times of QX-314 result in a stronger inhibition of sodium currents.[2] However, when we extended the application time of QX-314 in combination with capsaicin or carvacrol to 3 min or longer, the recordings became progressively instable such that a reliable estimation of sodium current inhibition by QX-314 as opposed to an unspecific rundown seemed inadequate (data not shown). Moreover, as is also demonstrated in figure 1, E and F, inward currents induced by both capsaicin (fig. 1E) and carvacrol (fig. 1F) displayed an almost complete tachyphylaxis within 60 s. When considering the hypothesis that QX-314 needs to permeate through the channel pores of TRPV1 and TRPA1 in order to inhibit sodium channels, it seems difficult to interpret any effects occurring after longer application times during which both TRPV1 and TRPA1 are inactivated.

As an alternative approach, we next examined a QX-314–mediated use-dependent block of sodium currents with or without coapplication of capsaicin or carvacrol (fig. 2). External application of 100 μM (6 ± 4%, n = 5) or 5 mM QX-314 (4 ± 3%, n = 7) did not result in a significant use-dependent block of Nav1.7 currents evoked by 100 depolarizing pulses from −120 to −10 mV at 10 Hz compared with control solution (5 ± 5%, n = 5; $P > 0.05$, Kruskal–Wallis with *post hoc* Dunn test; fig. 2C). When 100 μM QX-314 was added to the pipette solution, however, it induced a strong use-dependent block on currents activated at 10 Hz (54 ± 14%, n = 10; $P < 0.001$, Kruskal–Wallis with *post hoc* Dunn test; fig. 2, B and C). Thus, comparably low concentrations of intracellular QX-314 induce a pronounced use-dependent block of Nav1.7. We further investigated whether externally applied 5 mM QX-314 induces use-dependent block when hTRPV1 or hTRPA1 is activated by capsaicin or carvacrol. Application of 1 μM capsaicin alone did not result in a prominent use-dependent inhibition of sodium currents (7 ± 5%; n = 6; fig. 2, D and E). However, coapplication of capsaicin and 5 mM QX-314 resulted in a significant use-dependent block (34 ± 18%, n = 13; $P < 0.05$, Kruskal–Wallis with *post hoc* Dunn test; fig. 2, D and E). Similarly, 200 μM carvacrol in combination with 5 mM QX-314 produced a significantly stronger use-dependent block of sodium currents in cells expressing hTRPA1 compared with carvacrol alone (32 ± 8%, n = 8; carvacrol alone 6 ± 3%, n = 14; $P < 0.01$, Kruskal–Wallis with *post hoc* Dunn test; fig. 2, F and G). These data indicate that QX-314 can indeed permeate activated hTRPV1 and hTRPA1 channels to inhibit Nav1.7. In order to substantiate this finding, we next examined whether this use-dependent block is concentration dependent. Although application of 1 mM QX-314 together with capsaicin did not result in a significant use-dependent block (5 ± 11%, n = 7; $P > 0.05$, Kruskal–Wallis with *post hoc* Dunn test; fig. 2E), 30 mM QX-314 induced a strong use-dependent block (51 ± 30%, n = 7; $P < 0.01$, Kruskal–Wallis with *post hoc* Dunn test). A similar result was obtained on cells expressing hTRPA1, that is, 1 mM QX-314 (7 ± 17%, n = 6; $P > 0.05$, Kruskal–Wallis with *post hoc* Dunn test) failed to induce use-dependent block, whereas 30 mM QX-314 (45 ± 19%, n = 6;

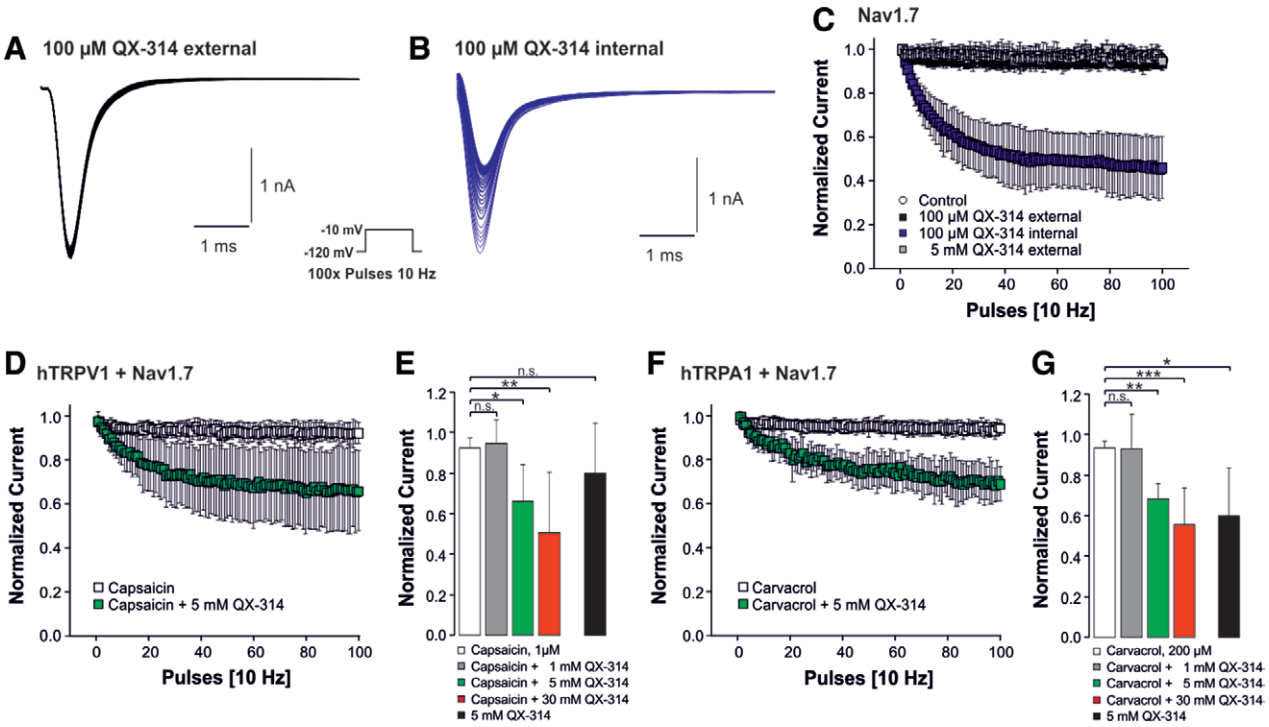

Fig. 2. QX-314 permeates through human (h) transient receptor potential vanilloid 1 (TRPV1) and human transient receptor potential cation channel, subfamily A, member 1 (TRPA1) channels to produce use-dependent block of sodium current. (*A*, *B*) Representative traces of sodium currents of Nav1.7 expressed in human embryonic kidney 293t (HEK-293t) lacking TRP channels. Currents were activated by 100 test pulses applied at 10 Hz in presence of 100 µM QX-314 in the extracellular solution (*A*) or the intracellular pipette solution (*B*). (*C*) Peak current amplitudes activated at 10 Hz were normalized to the amplitude of the first pulse and plotted against the pulse number. Note that although extracellular QX-314 at both 100 µM and 5 mM did not induce use-dependent block, 100 µM QX-314 in the pipette solution induced a strong use-dependent block. (*D*, *F*) Normalized peak current amplitudes activated at 10 Hz plotted against the pulse number in cells expressing hTRPV1 (*D*) and hTRPA1 (*F*) after the protocol described in figure 1D. (*E*, *G*) Bar diagrams displaying the effective inhibition of sodium currents at the last pulse after application of test substances. The peak amplitude of sodium currents activated after application of agonist ± QX-314 were normalized to the peak amplitudes of sodium currents determined at the first test pulse. Data are mean ± SD. n.s. = not significant, $^{*}P < 0.05$, $^{**}P < 0.01$, $^{***}P < 0.001$.

$P < 0.001$, Kruskal–Wallis with *post hoc* Dunn test; fig. 2G) produced a highly significant inhibition.

We finally explored whether permeation of QX-314 really requires preactivation of hTRPV1 or hTRPA1 channels by potent agonists. In cells expressing hTRPA1, application of only 5 mM QX-314 indeed produced a significant use-dependent block (40 ± 24%, n = 11; $P < 0.05$, Kruskal–Wallis with *post hoc* Dunn test; fig. 2G). In cells expressing hTRPV1, however, the weak use-dependent block observed after application of 5 mM QX-314 alone did not reach statistical significance (20 ± 25%, n = 9; $P > 0.05$, Kruskal–Wallis with *post hoc* Dunn test; fig. 2E).

QX-314 Activates TRPV1 and TRPA1

Our data suggest that, compared with rodent channels,[19,25] QX-314 might directly permeate or even gate human TRPV1 and TRPA1 channels. To examine this notion, we performed ratiometric calcium imaging and patch clamp recordings in hTRPV1- (fig. 3) and hTRPA1-expressing (fig. 4) cells. Indeed, a 40-s-long application of both 5 (fig. 3A) and 30 mM (fig. 3B) QX-314 induced an increase in intracellular calcium in cells expressing hTRPV1. In HEK-293 cells lacking TRPV1, however, we did not observe any effects by 5 or 30 mM QX-314 (fig. 3A, data shown only for 30 mM; n = 195). A lower percentage of cells expressing hTRPV1 responded to 30 mM QX-314 compared with 5 mM (5 mM: 100 ± 0.7% *vs.* 30 mM: 58 ± 27%; $P \leq 0.006$, Mann–Whitney U test, n = 7 to 13; fig. 3C), and the response to 30 mM QX-314 was significantly lower than to 5 mM QX-314 (AUC, 5 mM: 0.57 ± 0.18 *vs.* 30 mM: 0.17 ± 0.19; $P < 0.001$, ANOVA with Tukey *post hoc* test, n = 886 [5 mM] and 1,030 [30 mM], respectively; fig. 3D).

To confirm that the increase in intracellular calcium is due to activation of TRPV1 channels, we next monitored membrane currents during a 500-ms voltage ramp ranging from −100 to +100 mV (fig. 3E). QX-314 at 5 mM evoked slowly developing (more than 1 min) membrane currents with a strong outward rectification in all cells containing hTRPV1 (n = 11; fig. 3E), that is, inward currents at −100 mV (370 ± 616 pA) were small compared with

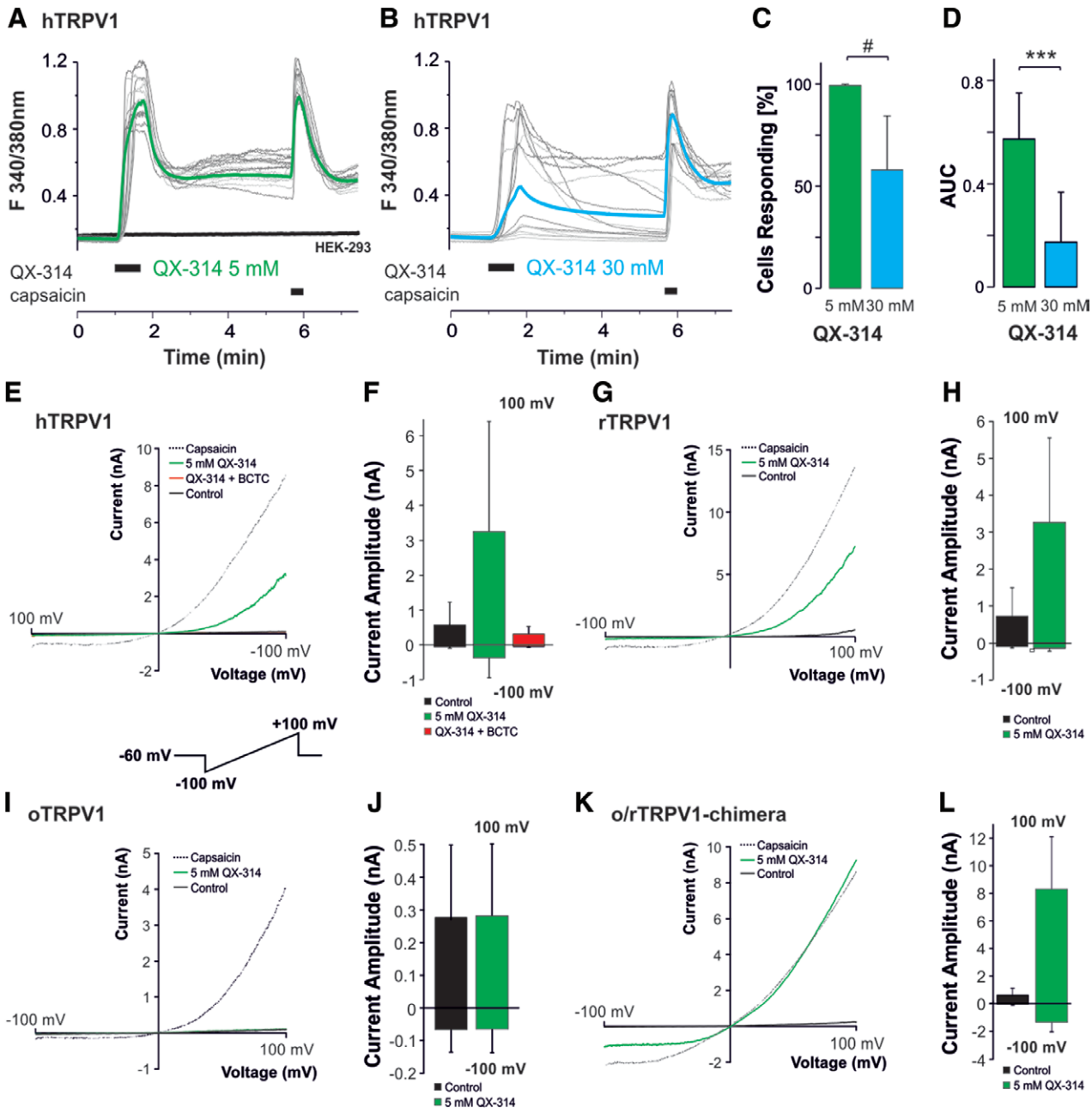

Fig. 3. QX-314 activates human (h) and rat (r) transient receptor potential vanilloid 1 (TRPV1) *via* the vanilloid-binding domain. (*A* and *B*) Mean responses of all measured cells with 5 mM (*A*, *green solid line*) and 30 mM (*B*, *blue solid line*) in cells expressing hTRPV1. Original traces from representative cells as displayed by *gray lines*, and the mean response of untransfected human embryonic kidney 293 (HEK-293) cells are displayed by the *black solid line* in *A*; 1 μM capsaicin was applied to verify the expression of hTRPV1. (*C*) Bar diagrams of the area under the curve (AUC) of fluorescence signals during the 60-s-long application of QX-314. (*D*) Bar diagram of the percentage of capsaicin-sensitive cells responding to QX-314 (***$P < 0.001$, ANOVA with Tukey *post hoc* test for AUC; and #$P \leq 0.006$, Mann–Whitney U test). (*E*, *G*, *I,* and *K*) Representative traces of QX-314–induced membrane currents in cells expressing (*E*) hTRPV1, (*G*) rTRPV1, (*I*) rabbit (o)TRPV1, and (*K*) the o/rTRPV1-chimera. Test solutions are listed in the panel. *Inset between E and I:* the recording protocol; currents were recorded during 500-ms voltage ramps from −100 to 100 mV in cells held at −60 mV. Capsaicin was applied at the end for each experiment as functional control for TRPV1 expression. Although capsaicin was usually applied 1 μM, the capsaicin-insensitive oTRPV1 required 10 μM capsaicin to generate robust membrane currents. Note that no membrane currents were activated upon coapplication of QX-314 with 100 nM 4-(3-chloro-2-pyridinyl)-*N*-[4-(1,1-dimethylethyl)phenyl]-1-piperazinecarboxamide (BCTC) (*E*). (*F*, *H*, *J*, and *L*) Bar diagrams of averaged (mean ± SD) peak amplitudes of membrane currents determined at −100 or 100 mV during application of different test solutions. Note that similar to capsaicin, QX-314–induced currents displayed a pronounced outward rectification, resulting in large outward currents at 100 mV. Also, note the 10-fold increase in y-axis scale in *J*, showing that oTRPV1 is not activated by QX-314. Data are mean ± SD, ratio of fluorescence intensity (F 340/380 nm).

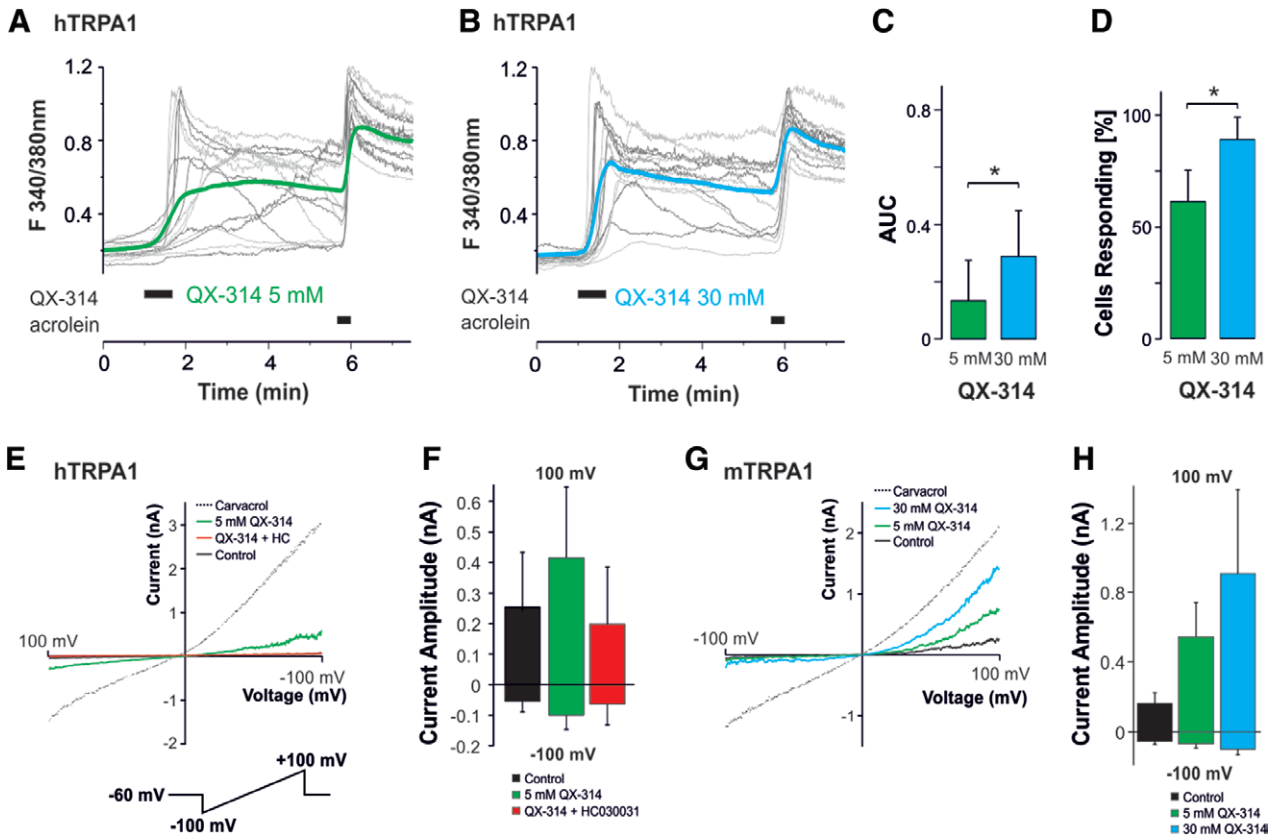

Fig. 4. QX-314 activates human (h) and mouse (m) transient receptor potential cation channel, subfamily A, member 1 (TRPA1). (*A* and *B*) Mean responses of all measured cells with 5 mM (*A*, *green solid line*) and 30 mM (*B*, *blue solid line*) and original traces from representative cells (*gray lines*); 50 μM acrolein was applied to verify expression of hTRPA1. (*C*) Bar diagram of the area under the curve (AUC) of fluorescence signals during the 60-s-long application of QX-314. (*D*) Bar diagram of the percentage of acrolein-sensitive cells responding to QX-314 (**P* < 0.05, ANOVA with Tukey *post hoc* test for AUC or Mann–Whitney U test for percentage). (*E*, *G*) Representative current traces of QX-314–induced membrane currents in cells expressing hTRPA1 (*E*) and mTRPA1 (*F*). All currents were recorded as described in figure 3. Carvacrol was applied at the end for each experiment as functional control for TRPA1 expression. Note that no membrane currents were observed when QX-314 was coapplied with 100 μM HC-030031 (*E*). (*F*, *H*) Bar diagrams displaying the corresponding average (mean ± SD) peak amplitudes of membrane currents determined at −100 or 100 mV during application of different test solutions as shown in *E* and *G*. Similar to TRPV1, TRPA1 generated QX-314–induced currents with a pronounced outward current. In cells expressing mTRPA1, 30 mM QX-314 induced larger membrane currents compared with 5 mM QX-314. **P* < 0.05, ratio of fluorescence intensity (F 340/380 nm).

outward currents at 100 mV (3,246 ± 3,004 pA; n = 11; fig. 3, E and F). Coapplication with the TRPV1 antagonist BCTC (100 nM) resulted in a complete inhibition of QX-314–induced currents (311 ± 223 pA at 100 mV; n = 8; fig. 3, E and F). QX-314 at 5 mM also activated rTRPV1 to a similar extent as hTRPV1 (inward: 132 ± 67 pA; outward: 3,265 ± 2,317 pA; n = 6; fig. 3, G and H). In a previous study, we demonstrated that lidocaine activates TRPV1 partly *via* interaction with the intracellular vanilloid-binding domain.[16] Therefore, we investigated whether this is also the case for QX-314. To that end, we explored the effects of QX-314 on the capsaicin-insensitive oTRPV1 that exhibits a very low vanilloid sensitivity.[16] QX-314 completely failed to induce membrane currents in cells expressing oTRPV1 (fig. 3, I and J; n = 8), such that both inward currents at −100 mV and outward currents at +100 mV did not increase after application of QX-314 (inward: 62 ± 75 pA; outward: 280 ± 225 pA) compared with control solution (inward: 64 ± 66 pA; outward: 276 ± 222 pA). These data suggest that QX-314 activates TRPV1 at least partly *via* interaction with the vanilloid-binding domain. We confirmed this notion by using a chimeric o/rTRPV1 construct in which the vanilloid-binding domain of oTRPV1 was replaced by the corresponding domain from rTRPV1. Indeed, 5 mM QX-314 induced prominent currents in this mutant (fig. 3, K and L, n = 7; inward: 1,364 ± 786 pA; outward: 8,293 ± 3,858 pA).

We further examined whether QX-314 also activates TRPA1. Acute application of 5 (fig. 4A) and 30 mM (fig. 4B) QX-314 for 40 s produced a significant increase of intracellular calcium in hTRPA1-expressing cells. Different from hTRPV1, 5 mM QX-314 evoked significantly smaller responses compared with 30 mM (AUC 5 mM: 0.13 ± 0.14;

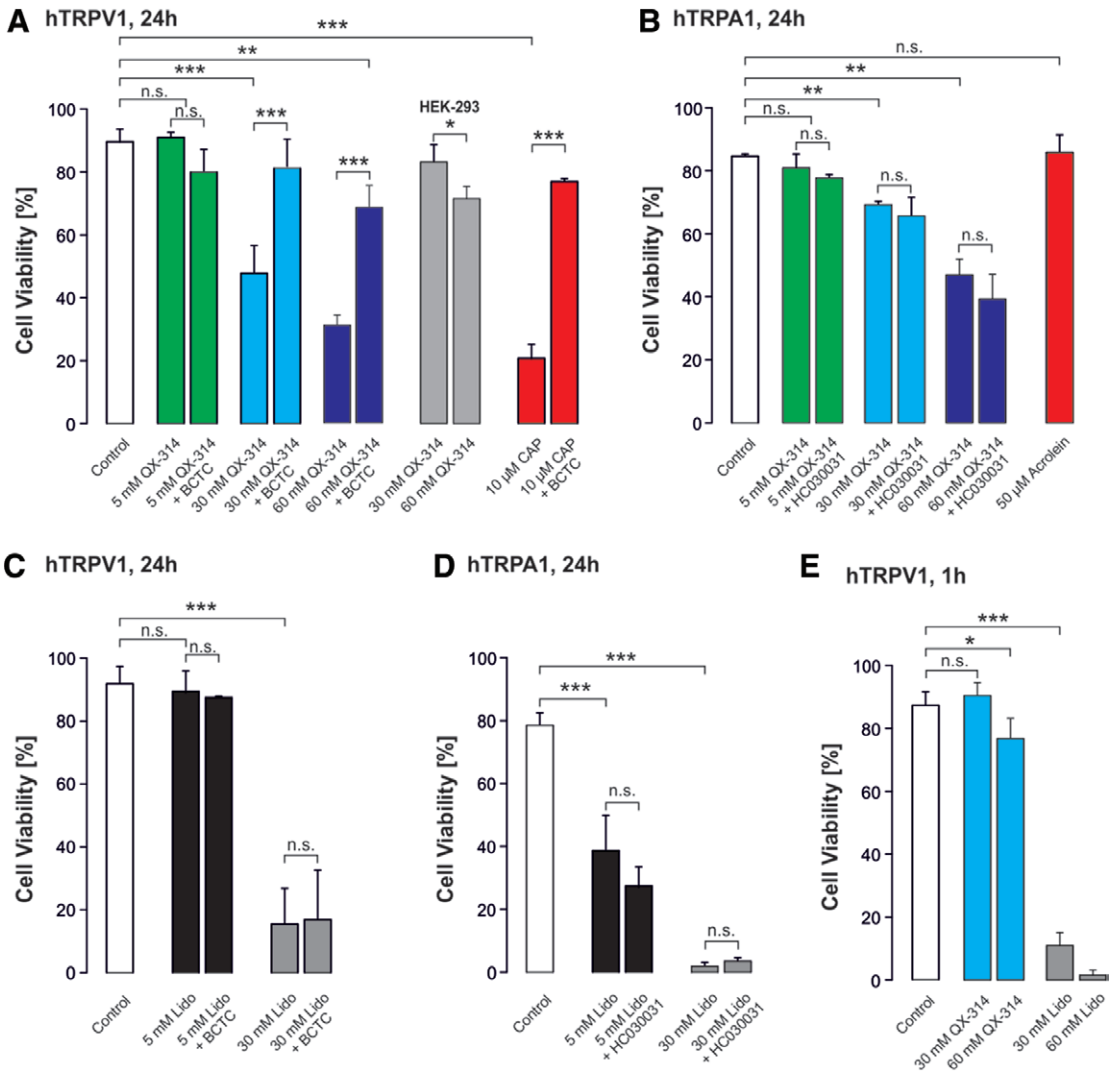

Fig. 5. QX-314 induces a transient receptor potential vanilloid 1 (TRPV1)-dependent cytotoxicity. (*A*) The fraction of viable human (h)TRPV1-expressing cells and native human embryonic kidney 293 (HEK-293) cells lacking TRP channels after incubation with different concentrations of QX-314 and capsaicin (CAP) with or without the TRPV1 antagonist 4-(3-chloro-2-pyridinyl)-*N*-[4-(1,1-dimethylethyl)phenyl]-1-piperazinecarboxamide (BCTC) (10 μM). (*B*) The fraction of viable human transient receptor potential cation channel, subfamily A, member 1 (hTRPA1)-expressing cells after incubation with different concentrations of QX-314 and acrolein with or without the TRPA1 antagonist HC-030031 (50 μM). (*C–E*) Viable hTRPV1- (*C*, *E*) and hTRPA1-expressing cells (*D*) incubated with different concentrations of lidocaine with and without BCTC (10 μM) and HC-030031 (50 μM), respectively. In *A* through *D*, cells were incubated for 15 min with substances, and cell death was assessed by staining after 24 h. In *E*, cell death was assessed after 1 h. Cells negative for annexin V and propidium iodide were considered viable. Data are mean ± SD. Statistical differences were assessed by one-way ANOVA with Tukey *post hoc* testing. **P* < 0.05, ***P* <0.01, ****P* < 0.001. n.s. = not significant.

AUC 30 mM: 0.29 ± 0.16, $P < 0.001$, n = 317 [5 mM] and 399 [30 mM], respectively; fig. 4C). Furthermore, the percentage of responding cells were higher when 30 mM of QX-314 was applied (5 mM: 62 ± 14%; 30 mM: 89 ± 10%, $P \leq 0.006$, Mann–Whitney U test, n = 7 to 13 experiments; fig. 4D). QX-314 at 5 mM also induced membrane current in cells expressing hTRPA1 (inward: 78 ± 58 pA; outward: 451 ± 192 pA; n = 10), and this effect was effectively inhibited by 50 μM of the TRPA1 antagonist HC-030031 (inward: 61 ± 70 pA; outward: 192 ± 186 pA; n = 6; fig. 4, E and F). Furthermore, we observed a concentration-dependent activation of mouse TRPA1 by 5 (inward: 69 ± 26 pA; outward: 544 ± 221 pA; n = 10) and 30 mM (inward: 100 ± 39 pA; outward: 910 ± 382 pA) QX-314 (fig. 4, G and H; n = 7). In analogy to a specific binding site of QX-314 in TRPV1, we hypothesized that QX-314 might activate TRPA1 *via* modification of intracellular N-terminal cysteins whose modulation is crucial for activation of TRPA1 by several reactive agonists including lidocaine.[19] However, the triple mutant hTRPA1-C621S/C641S/C665S generated robust QX-314–induced membrane currents both at 5 and 30 mM, suggesting that N-terminal cysteins are not the site of action of QX-314 in TRPA1 (data not shown).

QX-314 Induces TRPV1-dependent Cytotoxicity

Our data demonstrated that QX-314 directly activates TRPV1 and TRPA1 channels leading to a subsequent calcium influx (figs. 3A and 4A). It has been demonstrated that TRPV1-mediated calcium influx triggers apoptosis-like cascade leading to cell death.[22] We therefore evaluated the role of both TRP channels for cytotoxicity induced by QX-314 or lidocaine using double staining with annexin V FITC (annexin V) and PI with subsequent flow cytometric analysis (fig. 5). Cells negative for both substances (annexin V and PI) were defined as vital. We incubated the cells for 15 min with different concentrations of QX-314 and lidocaine or 1% PBS (control). After 15 min, substances were removed and cells recovered for 1 h (fig. 5E) or 24 h (fig. 5, A–D) before staining and flowcytometric analysis. Experiments were repeated three times. In hTRPV1-expressing HEK-293 cells, incubation with 5 mM QX-314 for 15 min did not induce a significant cell death, with 91 ± 2% surviving cells compared with control 90 ± 4% (fig. 5A). QX-314 at 30 mM induced a significant reduction of the viable cell fraction to 48 ± 8% ($P < 0.001$ compared with untreated control, ANOVA with Tukey *post hoc* test, n = 3). This effect was almost completely inhibited by coapplication of the TRPV1 antagonist BCTC (10 μM; 81 ± 9% viable cells; fig. 5A). QX-314 at 60 mM reduced the viable cell fraction to 31 ± 3%, but this effect was not completely inhibited by BCTC (68 ± 7%, $P < 0.01$ compared with control, ANOVA with Tukey *post hoc* test, n = 3). Cell death was not observed with 30 mM QX-314 (83 ± 5% viable cells) in TRPV1-negative HEK-293 cells, but 60 mM QX-314 induced cell death with a viable cell fraction of 70 ± 3% ($P < 0.01$ compared with control). In hTRPV1-expressing cells, incubation with 10 μM capsaicin induced significant cell death (21 ± 3% viable cells) compared with coincubation with 10 μ M capsaicin and 10 μM BCTC, resulting in significantly less cytotoxicity (77 ± 2% viable cells; $P < 0.001$, ANOVA with Tukey *post hoc*, n = 3).

In hTRPA1-expressing HEK-293 cells, neither 5 mM QX-314 nor 50 μM of the potent TRPA1 agonist acrolein induced a significant reduction of the viable cell fraction (fig. 5B). QX-314 at 30 mM reduced the viable cell fraction from 84 ± 1% in control to 69 ± 8%, and 60 mM QX-314 reduced viability to 47 ± 4%. This effect was not inhibited by the TRPA1 antagonist HC-030031 (50 μM). Similar to QX-314, 30 mM lidocaine reduced the amount of viable hTRPV1-expressing cells to 15 ± 11% (fig. 5C). However, this effect was not prevented by coincubation with BCTC (17 ± 16% viable cell fraction; fig. 5C). In hTRPA1-expressing cells, both 5 and 30 mM lidocaine induced significant cell death, 39 ± 10% and 2 ± 1%, respectively, of viable cells (fig. 5D). This effect was not reduced by the TRPA1 antagonist HC-030031 (27 ± 6% and 3 ± 1%, respectively; all $P < 0.001$ compared with control, ANOVA with Tukey *post hoc*).

We finally explored whether cell death mediated by hTRPV1 can be detected instantly after induction with QX-314 or lidocaine. Cells were incubated with tested substances for 15 min, and cell death was assessed after 1 h (fig. 5E); 60 mM, but not 30 mM, QX-314 reduced viability to 75 ± 6% ($P < 0.05$ compared with control). Both 30 and 60 mM lidocaine reduced the viable cell fraction to 11 ± 3% and 2 ± 2%, respectively. These data suggest that QX-314–induced cytotoxicity is in part mediated *via* TRPV1, but not *via* TRPA1.

Discussion

The current study adds new insights on the concept to introduce QX-314 into nociceptors *via* TRPV1 and TRPA1. QX-314 permeates the human isoforms of TRPV1 and TRPA1 to inhibit sodium channels. However, it also activates TRPV1 and TRPA1 to induce calcium influx, which in case of TRPV1 results in cytotoxicity.

Previous studies suggested that it is possible to use TRPV1 and TRPA1 as shuttles to take QX-314 into the cytosol of nociceptors.[27] The permeation of QX-314 through rodent TRPV1 with a subsequent local anesthesia was first demonstrated by Binshtok *et al.*[2] Later studies used various TRPV1 agonists in order to introduce QX-314 through TRPV1.[2,4,6,8,28,29] However, other reports demonstrated that QX-314 also induces a TRPV1-independent local anesthesia and even motor block by which TRPV1 agonists were not coadministered.[11,30,31] The ability of QX-314 to induce a motor block suggests that mechanisms other than TRPV1 and TRPA1 are used to induce a nerve conduction block. It is possible not only that extracellular QX-314 blocks voltage-gated ion channels other than sodium channels, but also that membrane proteins other than TRP channels allow entry of QX-314. Indeed, it was recently demonstrated that activation of the Toll-like receptor 5 in A-fibers allows entry of QX-314.[12] In contrast to TRPV1, comparably little has been published on the interaction of QX-314 with TRPA1. Although Nakagawa and Hiura[32] found that activation of TRPA1 by menthol does not enable permeation by QX-314, more recent studies indicate that activation of TRPA1 by allyl isothiocyanate, cinnamaldehyde, and bupivacaine enable permeation by QX-314.[9,10,33] Furthermore, it has become increasingly clear that several functional and pharmacological properties of TRPA1 and TRPV1 display significant species-specific differences between human and rodent isoforms.[11,12,30,31] As in most cases these differences are encoded by residues within the pore region; it is not clear that rodent and human isoforms share the ability to enable permeation of QX-314.

In contrast to previous studies on cultured sensory neurons, we failed to detect a significant reduction of the total sodium current by the combination of QX-314 and agonists compared with agonists or QX-314 alone. Application of both capsaicin and carvacrol resulted in a strong reduction of sodium currents. Similar effects were demonstrated for both TRPA1 and TRPV1 in cultured sensory neurons,[34] and they are probably partly explained by an increased intracellular sodium concentration due to the influx through TRP channels, and a consecutively reduced driving force for sodium through voltage-gated sodium channels.[35] However, this

possibility does not fully explain why we failed to establish a robust inhibition of sodium currents by introduction of QX-314. Whereas previous studies explored sodium currents in cells at holding potentials close to the physiological resting membrane potential (*i.e.*, −70 to −80 mV),[2,10,29] we performed our experiments at −120 mV. Nav1.7 underwent a considerable rundown when recordings were performed at −70 mV in our experiments, probably due to fast inactivation. Local anesthetics are known to have a low affinity to resting sodium channels,[1] and tonic block of resting Nav1.7 channels revealed an IC_{50} value of 1.7 mM. Assuming that intracellular lidocaine and QX-314 should be equipotent, this result indicates that a high intracellular concentration of QX-314 would be required to allow detection of tonic inhibition in our experiments. Binshtok *et al.*[4] observed a progressive reduction of sodium currents in sensory neurons treated with capsaicin and QX-314 for up to 25 min. Thus, it is possible that the application time (60 s) chosen in our study was too short. However, the quality of our recordings suffered substantially during such prolonged applications of capsaicin and carvacrol. We also observed that both TRPA1 and TRPV1 underwent a strong desensitization during 60 s, an effect that speaks against the notion that longer applications would allow more QX-314 to permeate through the channel pore. Instead, we show here that monitoring of use-dependent block offers a more reliable approach. The addition of 100 μM QX-314 in the pipette solution in cells lacking TRP channels resulted in a stronger use-dependent block compared with the effects induced by externally applied 5 mM QX-314 in cells expressing TRPV1 or TRPA1. Thus, our experimental protocol obviously resulted in an intracellular concentration of less than 100 μM QX-314.

In cells expressing hTRPA1, extracellularly applied QX-314 induced a prominent use-dependent block both with and without coapplication of carvacrol. Although not statistically significant, we also observed a small increase in use-dependent inhibition by application of QX-314 alone in cells expressing hTRPV1. This agonist-independent permeation of QX-314 through hTRPA1 and hTRPV1 was not described in any previous study. However, Puopolo *et al.*[36] observed that QX-314 permeates through TRPV1 without successive dilation of the channel pore. We demonstrate here that both TRPV1 and TRPA1 are activated by externally applied QX-314, that is, QX-314 seems to be able to permeate the channel pores to evoke activation of both TRPV1 and TRPA1. This finding may explain why QX-314 applied alone seems to induce local anesthetic effects as well as irritation in rodents.[11,20,37] However, it is also contradicting our previous studies demonstrating that QX-314 inhibits rather than activates rTRPV1 and hTRPA1.[19,25] Although in these studies QX-314 was only briefly (less than 20 s) applied to the cells, we now find that activation of both TRPV1 and TRPA1 develops slowly and results in rather small inward currents. A more recent study indeed demonstrated that QX-314 can both activate and inhibit rodent TRPV1.[7,38]

Our data indicate that activation of both TRPV1 and TRPA1 by QX-314 does not obey an obvious species specificity between human and rodent isoforms. Similar to what we previously described for lidocaine, experiments on constructs of the capsaicin-insensitive oTRPV1 channel suggest that QX-314 specifically interacts with the intracellularly located vanilloid-binding domain in order to gate TRPV1.[25] For TRPA1, however, QX-314 does not seem to interact with the intracellular cysteine residues known to be required for activation of several reactive TRPA1 agonists including lidocaine.[19] Thus, although the mechanism for activation of TRPV1 seems to require a permeation of the channel pore for QX-314 to reach the binding site, we can only assume that this is also the case for TRPA1.

The major finding of our study is that TRPV1 seems to be a relevant mediating mechanism of QX-314–induced cytotoxicity. Activation of TRPV1 by capsaicin and other agonists has been demonstrated to induce cytotoxic effects in neuronal and nonneuronal tissue.[22,39] Although the exact mechanisms of TRPV1-mediated cytotoxicity are unclear, most investigations indicate a calcium-mediated, apoptosis-like cell death.[22] It is also well established that clinically used local anesthetics induce neurotoxic effects.[24,40] Several mechanisms of local anesthetic–induced cytotoxicity have been suggested, including destruction of the outer cell membrane, activation of caspases, and disruption of the mitochondrial membrane.[23,40,41] QX-314 was recently suggested to induce significant neurotoxic effects after coapplication with lidocaine and capsaicin in rats.[5] In further murine *in vivo* experiments, very high concentrations of QX-314 (100 mM) induced detectable myotoxicity and soft tissue injury.[42] Toxic effects of QX-314 were also found after intrathecal[20] and IV injection[43] in rat *in vivo* models. In our study, cytotoxicity of 5 and 30 mM QX-314 was not apparent after a short investigation time of 1 h, which may indicate that activation of TRPV1 induces a regulated, time-dependent cellular death pathway. Although further studies are required to explore whether TRPV1 induces QX-314–induced neurotoxicity *in vivo*, this finding indicates that the desired permeation of QX-314 through TRPV1 may be directly associated with neurotoxicity. In contrast to QX-314, cytotoxicity of lidocaine was not mediated by TRPV1. Data reporting cytotoxic effects of lidocaine unrelated to cytosolic calcium levels support this notion.[44] Lidocaine may induce toxicity *via* TRPV1, but this effect is probably superimposed by other cytotoxic mechanisms described in literature.[40,41] As cytotoxicity of the clinically established local anesthetic lidocaine is considerably stronger and apparently also mediated by TRP channel–independent mechanisms, it may be that the toxic effects of QX-314 observed here are minor clinical relevance. However, unlike the membrane-permeable lidocaine that can readily be cleared from the cytosol *via* diffusion, it is possible that cytotoxicity induced by QX-314 is enhanced due to the fact that it is likely to be trapped in the cytosol for a longer time than lidocaine. Considering that both TRPV1 and TRPA1 mediate a strong calcium influx, we expected to

observe similar cytotoxic mechanisms *via* TRPA1. Although both QX-314 and lidocaine induced cytotoxic effects in hTRPA1-expressing cells, these effects were not prevented by the TRPA1-blocker HC-030031. Furthermore, activation of hTRPA1 by acrolein induced no cytotoxic effects. These data question the role of intracellular calcium as a key mechanism for cytotoxicity and rather suggest that other mechanisms downstream of TRPV1 are responsible for cytotoxicity. Nevertheless, if TRPV1 proves to mediate a relevant QX-314 neurotoxicity *in vivo*, our data indicate that an approach by which TRPA1 is selectively targeted may be associated with less or no neurotoxicity.

In summary, our results demonstrate a direct activation of human TRPV1 and TRPA1 by QX-314 with its subsequent permeation into the cytosol. Although this result suggests that QX-314 may be suited for selective sensory nerve blocks in humans, the associated neurotoxicity needs further evaluation.

Acknowledgments

The authors thank Heike Bürger for excellent technical assistance and Wolfgang Koppert, M.D., for continuous support (both from Department of Anaesthesiology and Intensive Care Medicine, Hannover Medical School, Hannover, Germany).

This study was supported by an Early Career Research Grant by the International Association for the Study of Pain (Washington, D.C.; 2012; to Dr. Leffler) and by the Wilhelm Sander-Stiftung (Munich, Germany; 2014.068.1; to Drs. Kistner and Reeh).

Competing Interests

The authors declare no competing interests.

Correspondence

Address correspondence to Dr. Stueber: Department of Anaesthesiology and Intensive Care Medicine, Hannover Medical School, Carl-Neuberg-Strasse 1, 30625 Hannover, Germany. stueber.thomas@mh-hannover.de. Information on purchasing reprints may be found at www.anesthesiology.org or on the masthead page at the beginning of this issue. Anesthesiology's articles are made freely accessible to all readers, for personal use only, 6 months from the cover date of the issue.

References

1. Nau C, Wang GK: Interactions of local anesthetics with voltage-gated Na^+ channels. J Membr Biol 2004; 201:1–8
2. Binshtok AM, Bean BP, Woolf CJ: Inhibition of nociceptors by TRPV1-mediated entry of impermeant sodium channel blockers. Nature 2007; 449:607–10
3. Roberson DP, Gudes S, Sprague JM, Patoski HA, Robson VK, Blasl F, Duan B, Oh SB, Bean BP, Ma Q, Binshtok AM, Woolf CJ: Activity-dependent silencing reveals functionally distinct itch-generating sensory neurons. Nat Neurosci 2013; 16:910–8
4. Binshtok AM, Gerner P, Oh SB, Puopolo M, Suzuki S, Roberson DP, Herbert T, Wang CF, Kim D, Chung G, Mitani AA, Wang GK, Bean BP, Woolf CJ: Coapplication of lidocaine and the permanently charged sodium channel blocker QX-314 produces a long-lasting nociceptive blockade in rodents. Anesthesiology 2009; 111:127–37
5. Peters CM, Ririe D, Houle TT, Aschenbrenner CA, Eisenach JC: Nociceptor-selective peripheral nerve block induces delayed mechanical hypersensitivity and neurotoxicity in rats. Anesthesiology 2014; 120:976–86
6. Ries CR, Pillai R, Chung CC, Wang JT, MacLeod BA, Schwarz SK: QX-314 produces long-lasting local anesthesia modulated by transient receptor potential vanilloid receptors in mice. Anesthesiology 2009; 111:122–6
7. Rivera-Acevedo RE, Pless SA, Ahern CA, Schwarz SK: The quaternary lidocaine derivative, QX-314, exerts biphasic effects on transient receptor potential vanilloid subtype 1 channels *in vitro*. Anesthesiology 2011; 114:1425–34
8. Zhou C, Liang P, Liu J, Zhang W, Liao D, Chen Y, Chen X, Li T: Emulsified isoflurane enhances thermal transient receptor potential vanilloid-1 channel activation-mediated sensory/nociceptive blockade by QX-314. Anesthesiology 2014; 121:280–9
9. Lennertz RC, Kossyreva EA, Smith AK, Stucky CL: TRPA1 mediates mechanical sensitization in nociceptors during inflammation. PLoS One 2012; 7:e43597
10. Brenneis C, Kistner K, Puopolo M, Jo S, Roberson D, Sisignano M, Segal D, Cobos EJ, Wainger BJ, Labocha S, Ferreirós N, von Hehn C, Tran J, Geisslinger G, Reeh PW, Bean BP, Woolf CJ: Bupivacaine-induced cellular entry of QX-314 and its contribution to differential nerve block. Br J Pharmacol 2014; 171:438–51
11. Lim TK, Macleod BA, Ries CR, Schwarz SK: The quaternary lidocaine derivative, QX-314, produces long-lasting local anesthesia in animal models *in vivo*. Anesthesiology 2007; 107:305–11
12. Xu ZZ, Kim YH, Bang S, Zhang Y, Berta T, Wang F, Oh SB, Ji RR: Inhibition of mechanical allodynia in neuropathic pain by TLR5-mediated A-fiber blockade. Nat Med 2015; 21:1326–31
13. Bianchi BR, Zhang XF, Reilly RM, Kym PR, Yao BB, Chen J: Species comparison and pharmacological characterization of human, monkey, rat, and mouse TRPA1 channels. J Pharmacol Exp Ther 2012; 341:360–8
14. Chen J, Kang D, Xu J, Lake M, Hogan JO, Sun C, Walter K, Yao B, Kim D: Species differences and molecular determinant of TRPA1 cold sensitivity. Nat Commun 2013; 4:2501
15. Chen J, Kym PR: TRPA1: The species difference. J Gen Physiol 2009; 133:623–5
16. Phillips E, Reeve A, Bevan S, McIntyre P: Identification of species-specific determinants of the action of the antagonist capsazepine and the agonist PPAHV on TRPV1. J Biol Chem 2004; 279:17165–72
17. Xiao B, Dubin AE, Bursulaya B, Viswanath V, Jegla TJ, Patapoutian A: Identification of transmembrane domain 5 as a critical molecular determinant of menthol sensitivity in mammalian TRPA1 channels. J Neurosci 2008; 28:9640–51
18. de la Roche J, Eberhardt MJ, Klinger AB, Stanslowsky N, Wegner F, Koppert W, Reeh PW, Lampert A, Fischer MJ, Leffler A: The molecular basis for species-specific activation of human TRPA1 protein by protons involves poorly conserved residues within transmembrane domains 5 and 6. J Biol Chem 2013; 288:20280–92
19. Leffler A, Lattrell A, Kronewald S, Niedermirtl F, Nau C: Activation of TRPA1 by membrane permeable local anesthetics. Mol Pain 2011; 7:62
20. Schwarz SK, Cheung HM, Ries CR, Lee SM, Wang JT, MacLeod BA: Lumbar intrathecal administration of the quaternary lidocaine derivative, QX-314, produces irritation and death in mice. Anesthesiology 2010; 113:438–44
21. Lumpkin EA, Caterina MJ: Mechanisms of sensory transduction in the skin. Nature 2007; 445:858–65

22. Davies JW, Hainsworth AH, Guerin CJ, Lambert DG: Pharmacology of capsaicin-, anandamide-, and N-arachidonoyl-dopamine-evoked cell death in a homogeneous transient receptor potential vanilloid subtype 1 receptor population. Br J Anaesth 2010; 104:596–602
23. Lirk P, Haller I, Myers RR, Klimaschewski L, Kau YC, Hung YC, Gerner P: Mitigation of direct neurotoxic effects of lidocaine and amitriptyline by inhibition of p38 mitogen-activated protein kinase *in vitro* and *in vivo*. Anesthesiology 2006; 104:1266–73
24. Perez-Castro R, Patel S, Garavito-Aguilar ZV, Rosenberg A, Recio-Pinto E, Zhang J, Blanck TJ, Xu F: Cytotoxicity of local anesthetics in human neuronal cells. Anesth Analg 2009; 108:997–1007
25. Leffler A, Fischer MJ, Rehner D, Kienel S, Kistner K, Sauer SK, Gavva NR, Reeh PW, Nau C: The vanilloid receptor TRPV1 is activated and sensitized by local anesthetics in rodent sensory neurons. J Clin Invest 2008; 118:763–76
26. Stoetzer C, Kistner K, Stüber T, Wirths M, Schulze V, Doll T, Foadi N, Wegner F, Ahrens J, Leffler A: Methadone is a local anaesthetic-like inhibitor of neuronal Na^+ channels and blocks excitability of mouse peripheral nerves. Br J Anaesth 2015; 114:110–20
27. Roberson DP, Binshtok AM, Blasl F, Bean BP, Woolf CJ: Targeting of sodium channel blockers into nociceptors to produce long-duration analgesia: A systematic study and review. Br J Pharmacol 2011; 164:48–58
28. Price TJ, Patwardhan AM, Flores CM, Hargreaves KM: A role for the anandamide membrane transporter in TRPV1-mediated neurosecretion from trigeminal sensory neurons. Neuropharmacology 2005; 49:25–39
29. Liu H, Zhang HX, Hou HY, Lu XF, Wei JQ, Wang CG, Zhang LC, Zeng YM, Wu YP, Cao JL: Acid solution is a suitable medium for introducing QX-314 into nociceptors through TRPV1 channels to produce sensory-specific analgesic effects. PLoS One 2011; 6:e29395
30. Hofmann ME, Largent-Milnes TM, Fawley JA, Andresen MC: External QX-314 inhibits evoked cranial primary afferent synaptic transmission independent of TRPV1. J Neurophysiol 2014; 112:2697–706
31. Zhao Y, Zhou C, Liu J, Liang P, Liao D, Chen Y, Chen X: The quaternary lidocaine derivative QX-314 produces long-lasting intravenous regional anesthesia in rats. PLoS One 2014; 9:e99704
32. Nakagawa H, Hiura A: Comparison of the transport of QX-314 through TRPA1, TRPM8, and TRPV1 channels. J Pain Res 2013; 6:223–30
33. Chen J, Kim D, Bianchi BR, Cavanaugh EJ, Faltynek CR, Kym PR, Reilly RM: Pore dilation occurs in TRPA1 but not in TRPM8 channels. Mol Pain 2009; 5:3
34. Andersson DA, Gentry C, Alenmyr L, Killander D, Lewis SE, Andersson A, Bucher B, Galzi JL, Sterner O, Bevan S, Högestätt ED, Zygmunt PM: TRPA1 mediates spinal antinociception induced by acetaminophen and the cannabinoid Δ(9)-tetrahydrocannabiorcol. Nat Commun 2011; 2:551
35. Onizuka S, Yonaha T, Tamura R, Hosokawa N, Kawasaki Y, Kashiwada M, Shirasaka T, Tsuneyoshi I: Capsaicin indirectly suppresses voltage-gated Na^+ currents through TRPV1 in rat dorsal root ganglion neurons. Anesth Analg 2011; 112:703–9
36. Puopolo M, Binshtok AM, Yao GL, Oh SB, Woolf CJ, Bean BP: Permeation and block of TRPV1 channels by the cationic lidocaine derivative QX-314. J Neurophysiol 2013; 109:1704–12
37. Shen J, Fox LE, Cheng J: Differential effects of peripheral *versus* central coadministration of QX-314 and capsaicin on neuropathic pain in rats. Anesthesiology 2012; 117:365–80
38. Rivera-Acevedo RE, Pless SA, Schwarz SK, Ahern CA: Expression-dependent pharmacology of transient receptor potential vanilloid subtype 1 channels in *Xenopus laevis* oocytes. Channels (Austin) 2013; 7:47–50
39. Stock K, Kumar J, Synowitz M, Petrosino S, Imperatore R, Smith ES, Wend P, Purfürst B, Nuber UA, Gurok U, Matyash V, Wälzlein JH, Chirasani SR, Dittmar G, Cravatt BF, Momma S, Lewin GR, Ligresti A, De Petrocellis L, Cristino L, Di Marzo V, Kettenmann H, Glass R: Neural precursor cells induce cell death of high-grade astrocytomas through stimulation of TRPV1. Nat Med 2012; 18:1232–8
40. Werdehausen R, Braun S, Essmann F, Schulze-Osthoff K, Walczak H, Lipfert P, Stevens MF: Lidocaine induces apoptosis *via* the mitochondrial pathway independently of death receptor signaling. Anesthesiology 2007; 107:136–43
41. Onizuka S, Tamura R, Yonaha T, Oda N, Kawasaki Y, Shirasaka T, Shiraishi S, Tsuneyoshi I: Clinical dose of lidocaine destroys the cell membrane and induces both necrosis and apoptosis in an identified Lymnaea neuron. J Anesth 2012; 26:54–61
42. Shankarappa SA, Sagie I, Tsui JH, Chiang HH, Stefanescu C, Zurakowski D, Kohane DS: Duration and local toxicity of sciatic nerve blockade with coinjected site 1 sodium-channel blockers and quaternary lidocaine derivatives. Reg Anesth Pain Med 2012; 37:483–9
43. Cheung HM, Lee SM, MacLeod BA, Ries CR, Schwarz SK: A comparison of the systemic toxicity of lidocaine *versus* its quaternary derivative QX-314 in mice. Can J Anaesth 2011; 58:443–50
44. Doan LV, Eydlin O, Piskoun B, Kline RP, Recio-Pinto E, Rosenberg AD, Blanck TJ, Xu F: Despite differences in cytosolic calcium regulation, lidocaine toxicity is similar in adult and neonatal rat dorsal root ganglia *in vitro*. Anesthesiology 2014; 120:50–61